# Mode Competition and Anomalous Cooling in a Multimode Phonon Laser

Utku Kemiktarak,[1,2] Mathieu Durand,[2] Michael Metcalfe,[1,2] and John Lawall[2]
[1]Joint Quantum Institute, University of Maryland, College Park, Maryland 20742, USA
[2]National Institute of Standards and Technology, 100 Bureau Drive, Gaithersburg, Maryland 20899, USA
(Received 13 August 2013; revised manuscript received 14 February 2014; published 15 July 2014)

We study mode competition in a multimode "phonon laser" comprised of an optical cavity employing a highly reflective membrane as the output coupler. Mechanical gain is provided by the intracavity radiation pressure, to which many mechanical modes are coupled. We calculate the gain and find that strong oscillation in one mode suppresses the gain in other modes. For sufficiently strong oscillation, the gain of the other modes actually switches sign and becomes damping, a process we call "anomalous cooling." We demonstrate that mode competition leads to single-mode operation and find excellent agreement with our theory, including anomalous cooling.

DOI: 10.1103/PhysRevLett.113.030802 PACS numbers: 07.10.Cm, 42.50.Wk, 42.55.Ah, 42.79.Dj

*Introduction.*—While the laser was invented more than five decades ago, its acoustic analog has only recently been realized. Following the observation of phonon amplification in microwave-pumped ruby [1] in 1961 came the suggestion of "phonon lasing." Subsequent work in ruby studied the emission spectrum of phonon generation [2] and multimode processes [3]. Alternative platforms for a phonon laser were studied as well, including experimental work with optically pumped heterostructures [4] and theoretical studies of electrically pumped heterostructures [5,6]. Electrically pumped phonon emission was observed in a semiconductor superlattice [7], and the amplification and spectral narrowing characteristic of stimulated emission were demonstrated [8]. In parallel, resonant cavities for phonons in semiconductor heterostructures were realized [9]. With the advent of optical pumping, detailed studies of the coherence of phonon emission in ruby were enabled [10], culminating in a ruby "saser" (sound amplification by stimulated emission of radiation) [11]. Shortly thereafter, phonon lasing was realized in a harmonically bound $Mg^+$ ion driven by optical forces [12].

Subsequently, it was recognized that optomechanical systems in which optically furnished gain enables self-sustained mechanical oscillation are properly called "phonon lasers" [13]. These include beams [13,14] and cantilevers [15] coupled to an optical cavity, microtoroids [16,17], and a cantilever deriving mechanical gain from optical band gap excitation [18]. Analogous electromechanical [19,20] and purely mechanical [21] systems have also been discussed. Various phenomena associated with lasers, such as stimulated emission [12], oscillation threshold [12,13,17,18,21], gain narrowing [21], and injection locking [22], have been demonstrated.

With few exceptions, these investigations have involved a single mechanical mode. Multimode emission was observed in ruby [2,3], and two-mode oscillation was observed in a photothermally coupled optomechanical system [15]. Intermodal coupling in an electromechanical system was exploited to realize a phonon laser without an optical pump [21]. In the domain of conventional lasers, an interesting and important feature arises when multimode operation is considered. As shown by Lamb in 1964 [23], a saturation phenomenon occurs in which the oscillation of one mode suppresses the gain of other modes. This has the dramatic consequence that, in the absence of inhomogeneous gain broadening, a laser oscillates in a steady state on a single mode, even when the small-signal gain exceeds the losses for more than one mode [24,25]. Indeed, monochromatic output is one of the most notable and useful characteristics of laser light.

In view of the multimode oscillation observed in the photothermal system [15], it is natural to ask whether a phonon laser employing pure radiation pressure coupling would exhibit the single-mode oscillation characteristic of a homogeneously broadened laser. Here, we study such a system, in which one cavity mirror is formed by a highly reflective membrane supporting many mechanical modes. We find that when the mechanical gain exceeds the losses for more than one mode, the steady-state condition is nevertheless always that of a single oscillating mode. We calculate the gain for the case of two modes and find that, just as in the conventional laser, a strongly oscillating mode tends to "steal" gain from competing modes. Sufficient oscillation amplitude, in fact, reverses the sign of the gain of more weakly oscillating modes, causing them to be optically damped. Experimentally, we are able to force certain modes to oscillate, or to put the system in a regime in which the mode that ultimately oscillates is unpredictable and depends on thermal fluctuations. In addition, we verify our prediction that as the oscillation strength of one mode is increased, the quenched modes are, in fact, cooled.

*Experiment.*—As illustrated in Fig. 1, our optomechanical resonator is used as the output coupler of a Fabry-Perot cavity. It is a square (side $a = 1.25$ mm) silicon nitride membrane, patterned with an array of gratings, each 50 $\mu$m

 

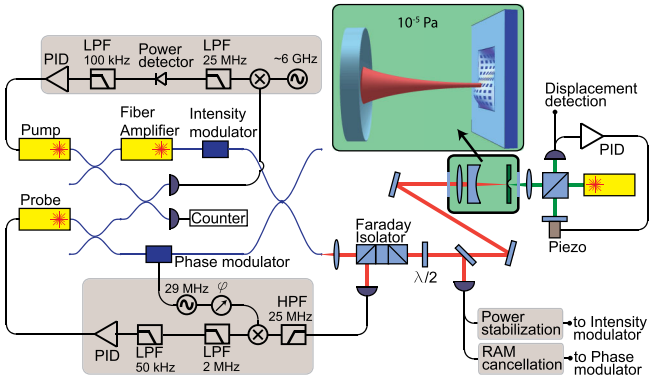


FIG. 1 (color online). A Fabry-Perot cavity employing a highly reflective subwavelength grating in a silicon nitride membrane, operated in vacuum, forms the optomechanical system. A "probe" laser is locked to a cavity resonance, while a "pump" laser is blue detuned relative to the adjacent longitudinal cavity resonance and provides mechanical gain. A third laser is used for a Michelson interferometer to sense membrane displacements. PID is the proportional-integral-derivative controller, HPF is high-pass filter, and LPF is low-pass filter.

on a side. Each grating has a period smaller than the wavelength (1.56 $\mu$m) of the light and has near-unity reflectivity. The optomechanical properties of the device have previously been reported [26,27]. Only one of the gratings is used at a time, but by choosing a particular grating, one can optimize the radiation pressure coupling to a certain set of mechanical modes. All of the results in this paper employ a grating centered at $x_0 = 465(10)$ $\mu$m and $y_0 = 400(10)$ $\mu$m relative to a membrane corner. The reflectivity of this particular grating yields a cavity finesse $F \approx 1000$. The input coupler has a radius of curvature of $R = 25$ mm. We use a cavity length $L_{\rm cav} \approx R$ so that the waist $\omega_0$ of the optical mode is below 20 $\mu$m; correspondingly, the cavity free spectral range is $\Delta\nu \approx 6$ GHz.

We introduce two lasers into the cavity: a probe laser and a pump laser, both with $\lambda = 1.56$ $\mu$m, as shown in Fig. 1. The probe laser is locked to a cavity resonance; the pump is frequency offset from the probe laser by $\Delta\nu + \delta\nu$, where $\delta\nu$ represents an arbitrary detuning from the adjacent cavity mode. In order to transduce membrane displacements, we implement a Michelson interferometer targeting the grating used for the optical cavity. The Michelson beam employs a third laser at 1.56 $\mu$m that is far off resonance from any cavity mode (cavity linewidth≈6 MHz).

*Radiation pressure-induced dynamics.*—The power circulating in the Fabry-Perot cavity is correlated to the membrane motion, optically modifying the dynamics. The case of a single mechanical mode has been studied extensively [16]; the radiation pressure enables optically modified frequency shifts, cooling, and oscillation. Here, we generalize to multiple mechanical modes. We express the membrane displacement $z(x, y, t)$ as a sum of products of normal modes $\phi_{mn}(x, y)$ with time-dependent factors $q_{mn}(t)$: $z(x, y, t) = \sum_{m,n} q_{mn}(t)\phi_{mn}(x, y)$. For a uniform square membrane, the modes are given by $\phi_{mn}(x, y) = \sin(m\pi x/a)\sin(n\pi y/a)$, and the effective mass $m_{\rm eff}$ is equal to one-fourth of the membrane mass [28]. Each mode is driven by generalized force $F_{mn}(t) = \int\int f(x, y, t)\phi_{mn}(x, y)dxdy$ [28], where $f(x, y, t)$ is the radiation pressure force per unit area.

The amplitude $u(t)$ of the electric field circulating in a high-finesse Fabry-Perot cavity with a varying cavity length $L(t) = L_0 + z(t)$ is governed by the differential equation

$$\dot{u}(t) + \left[\gamma - i\left(\delta\omega + \frac{4\pi z(t)}{\lambda}\Delta\nu\right)\right]u(t) = i\Delta\nu\sqrt{T_1 P_{\rm in}}, \quad (1)$$

where $\Delta\nu = c/(2L_0)$, $\gamma$ is the cavity field decay rate, related to the finesse $F$ by $\gamma = \pi\Delta\nu/F$, and $T_1$ is the transmission of the input coupler. The cavity is driven by laser light of frequency $\nu_L$, wavelength $\lambda$, and power $P_{\rm in}$, detuned from a resonance frequency $\nu_0$ by $\delta\omega = 2\pi\delta\nu = 2\pi(\nu_L - \nu_0)$. The intensity distribution is Gaussian, with spot size $\omega_0$, centered at $(x_0, y_0)$.

For a sinusoidal membrane oscillation $q_{mn}(t) \equiv z_{mn}\sin 2\pi\nu_{mn}t$, the solution to Eq. (1) contains a spectrum of sidebands separated by $\nu_m$. The dimensionless quantity $\chi_{mn} \equiv 2(\Delta\nu/\nu_{mn})(z_{mn}/\lambda)\phi_{mn}(x_0, y_0)$ appears as a natural expansion parameter and, for $\chi_{mn} > 1$, corresponds roughly to the number of sidebands with significant amplitude. The radiation pressure $F^{\rm RP} = 2|u(t)|^2/c$ associated with the circulating optical power oscillates at $\nu_{mn}$ and all of its harmonics. For a high-$Q$ mechanical oscillator, the dynamics are well described by

$$\ddot{q}_{mn} + [\Gamma^{\rm intr}_{mn} + \Gamma^{\rm RP}_{mn}(\{\chi_{rs}\})]\dot{q}_{mn} + \omega^2_{mn}q_{mn} = \frac{F_{\rm th}(t)}{m_{\rm eff}}. \quad (2)$$

Here, $\omega_{mn} = 2\pi\nu_{mn}$, and $\Gamma^{\rm intr}_{mn}$ is the intrinsic damping of mode $mn$, related to the mechanical quality factor $Q_{mn}$ by $\Gamma^{\rm intr}_{mn} = \omega_{mn}/Q_{mn}$. $F_{\rm th}(t)$ is the thermal Langevin force, with spectral density $S_F(\omega) = 4k_B T m_{\rm eff}\Gamma^{\rm intr}_{mn}$. The $\Gamma^{\rm RP}_{mn}(\{\chi_{rs}\})$ are optical modifications to the damping of mode $mn$; modifications to the $\omega_{mn}$ are also present but not significant here. In general, $\Gamma^{\rm RP}_{mn}(\{\chi_{rs}\})$ depends on the set of amplitudes $\{\chi_{rs}\}$ of all of the modes.

If the amplitudes are all small ($\chi_{mn} \ll 1$), only the first-order sidebands need be considered. In this case, $\Gamma^{\rm RP}_{mn}$ can be shown to be independent of the $\{\chi_{rs}\}$, and the optical damping works independently for each mode. In previous work, we have optically cooled hundreds of mechanical modes simultaneously [27].

The situation $\Gamma^{\rm RP}_{mn} < 0$ corresponds to antidamping, or optically furnished mechanical gain, and is obtained by blue detuning ($\delta\nu > 0$). If the optical gain exceeds the intrinsic damping $-\Gamma^{\rm RP}_{mn} > \Gamma^{\rm intr}_{mn}$, the amplitude rings up from its thermal value, and the first-order theory loses validity. Indeed, as the amplitude of each mode grows, it

suppresses the gain of all of the other modes as determined by the rates $\Gamma^{\mathrm{RP}}_{mn}(\{\chi_{rs}\})$. This phenomenon of intermode gain suppression has a dramatic signature: it causes an antidamped system to oscillate on a single mode, even if the unsaturated mechanical gain exceeds the oscillation threshold for more than one mode.

To see this, we start by calculating $\Gamma^{\mathrm{RP}}$ for the case of two low-order nondegenerate modes, where we use the letters $A$ and $B$ to label mode indices $mn$. For $\omega_0 \ll a$, we find (see the Supplemental Material [29]) the gain of mode $A$ to be

$$\Gamma^{\mathrm{RP}}_A(\chi_A,\chi_B) = \mathcal{C}P_{\mathrm{in}}\left(\frac{\phi_A^2(x_0,y_0)}{\nu_A^2}\right)\times \mathrm{Im}\left\{\frac{1}{\chi_A}\sum_{k,l=-\infty}^{\infty}\frac{J_k(\chi_A)J_{k-1}(\chi_A)}{\gamma - i[\delta\omega-(k\omega_A+l\omega_B)]}\frac{J_l^2(\chi_B)}{\gamma+i\{\delta\omega-[(k-1)\omega_A+l\omega_B]\}}\right\},$$

where $\chi_A$ and $\chi_B$ describe the oscillation amplitudes, $\mathcal{C} = 4T_1\Delta\nu^3/(\pi m_{\mathrm{eff}}\lambda c)$, and the $J_k$ are Bessel functions. Clearly, the gain of mode $A$ depends on the oscillation amplitude of mode $B$. The single-mode case, which we consider initially, can be obtained by taking $\chi_B \to 0$, $\Gamma^{\mathrm{RP}}_A(\chi_A) \equiv \Gamma^{\mathrm{RP}}_A(\chi_A,0)$.

The single-mode oscillation threshold condition is given by $\Gamma^{\mathrm{RP}}_A(0) = -\Gamma^{\mathrm{intr}}_A$, and the steady-state oscillation amplitude $\chi_A$ is given by $\Gamma^{\mathrm{RP}}_A(\chi_A) = -\Gamma^{\mathrm{intr}}_A$. Figure 2 shows (red curve) the gain of mode $(m,n) = (2,1)$ normalized to its small-amplitude value $\Gamma^{\mathrm{RP}}_{21}(\chi_{21})/\Gamma^{\mathrm{RP}}_{21}(0)$. We have taken a detuning of $\delta\omega = 0.67\gamma$ and a mechanical frequency of $\omega_{21} = 0.07\gamma$, corresponding to values used in our experiment. This curve shows gain saturation, as expected: $\Gamma^{\mathrm{RP}}$ drops to half of the small-amplitude value for an oscillation amplitude of $\chi \approx 16$.

*Mode competition.*—More interesting phenomena arise when we consider how the gain of mode (1,2) is affected by the amplitude of mode (2,1). Figure 2 (blue curve) shows the gain of the (1,2) mode, in the limit of small oscillation amplitude $\chi_{12}$, as a function of $\chi_{21}$. The curve exhibits two key features: the gain of the weakly oscillating mode (1,2) diminishes more rapidly with amplitude $\chi_{21}$ than that of the stronger mode (2,1), and, when the (2,1) mode oscillates with $\chi_{21} > 18$, the gain of the weak mode actually switches sign and provides damping. Qualitatively similar behavior (not shown) is found for the gain of the (2,1) mode as a function of $\chi_{12}$.

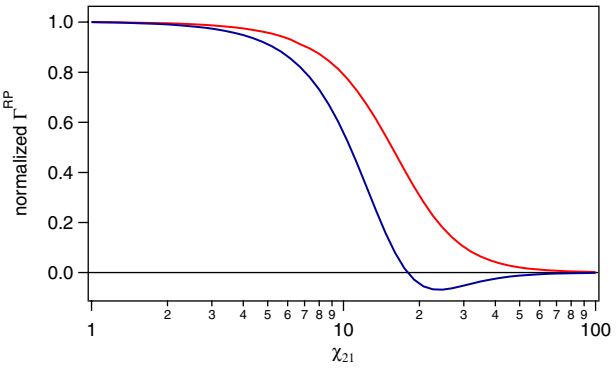


FIG. 2 (color online). Gain saturation vs oscillation amplitude, calculated for detuning $\delta\omega = 0.67\gamma$. Red curve: single-mode normalized antidamping $\Gamma^{\mathrm{RP}}_{21}(\chi_{21})/\Gamma^{\mathrm{RP}}_{21}(0)$ of mode (2,1) vs dimensionless amplitude $\chi_{21}$. Blue curve: two-mode normalized (anti)damping of mode (1,2) when it is oscillating weakly $\Gamma^{\mathrm{RP}}_{12}(0,\chi_{21})/\Gamma^{\mathrm{RP}}_{12}(0,0)$ for arbitrary $\chi_{21}$. The gain of the (1,2) mode switches sign for large $\chi_{21}$.

In our experiment, the mode with the lowest threshold power is the (1,2) mode, with $\nu_{12} = 192$ kHz, $\Gamma^{\mathrm{intr}}_{12} = 2.5(2)\ \mathrm{s}^{-1}$, and geometrical coupling $\phi_{1,2}(x_0,y_0) = 0.62(3)$. The (2,1) mode, with $\nu_{21} = 207$ kHz, $\Gamma^{\mathrm{intr}}_{21} = 4.8(3)\ \mathrm{s}^{-1}$, and $\phi_{2,1}(x_0,y_0) = 0.83(2)$, has a slightly higher threshold power $P^{\mathrm{thresh}}_{2,1} = 1.05P^{\mathrm{thresh}}_{1,2}$, so for incident laser power $P^{\mathrm{thresh}}_{1,2} < P_{\mathrm{in}} < P^{\mathrm{thresh}}_{2,1}$, the (1,2) mode is the only one that will oscillate. The (2,1) mode is, however, better coupled to the radiation pressure, and for $P_{\mathrm{in}} \gg P^{\mathrm{thresh}}_{2,1}$, the net small-amplitude gain $-[\Gamma^{\mathrm{RP}}_{21}(\{\chi^{\mathrm{thermal}}_{rs}\}) + \Gamma^{\mathrm{intr}}_{21}]$ is found to be 1.8 times larger than the corresponding gain for the (1,2) mode. For large pump powers, then, the (2,1) mode more quickly rings up from thermal amplitude, and as it does, the gain for the more weakly oscillating (1,2) mode is suppressed, as indicated in Fig. 2. Thus, by appropriate choice of pump power, it is possible to deterministically force either the (1,2) or (2,1) mode to oscillate. With different experimental parameters, we have similarly been able to force the (1,1) and (2,2) modes to oscillate.

For pump powers exceeding the oscillation threshold of both modes (1,2) and (2,1), but low enough that the net small-amplitude gains for the two modes are comparable, it is not possible to predict which mode will oscillate in the steady state. We study the time dependence of the mode competition by sending the signal from the Michelson interferometer into lock-in amplifiers referenced to $\nu_{12}$ and $\nu_{21}$. Figures 3(a) and 3(b) (solid lines) show typical amplitudes $z_{mn}(t)$ for such experiments. We switch on the pump at time $t \approx 50$ s, with detuning $\delta\omega = 0.67\gamma$ and power slightly larger than $P^{\mathrm{thresh}}_{2,1}$, and switch it back off at $t \approx 175$ s. The amplitudes of the (1,2) and (2,1) modes both initially grow, but after several seconds, one mode grows until its gain is saturated, while the growth of the other mode is quenched. Independent measurements confirm that the oscillations of all other modes are likewise quenched.

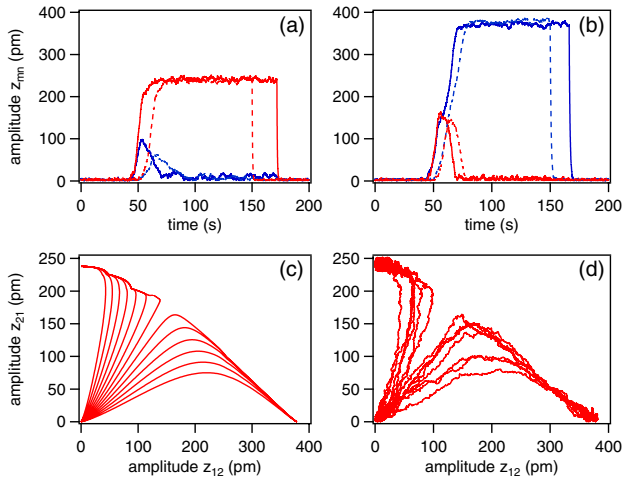


FIG. 3 (color online). (a),(b) Time dependence of mode competition between (1,2) and (2,1) modes, where the outcome is unpredictable. Blue curves: (1,2) mode. Red curves: (2,1) mode. Solid lines: experiment; the pump is turned on at $t \approx 50$ s and turned off at $t \approx 175$ s. Dashed lines: simulations; the pump on and off times are slightly different for clarity. (c) Set of simulations for slightly different initial conditions; no thermal excitation. (d) Measured set of 13 trajectories such as those shown in (a) and (b).

From the amplitudes of the steady-state oscillation in Figs. 3(a) and 3(b) (75 s $< t <$ 175 s), we infer $\chi_{21} = 7.4$ and $\chi_{12} = 9.2$, respectively. From the calculated dependence of gains on $\chi_{21}$ (Fig. 2) and $\chi_{12}$, one infers $P_{\rm in} = 1.18(2)P_{1,2}^{\rm thresh}$, and one also finds the net damping $\Gamma_{mn}^{\rm net} = \Gamma_{mn}^{\rm intr} + \Gamma_{mn}^{\rm RP}(\{\chi_{rs}\})$ of the modes that are quenched to be $\Gamma_{12}^{\rm net} \approx 0.2\ {\rm s}^{-1}$ and $\Gamma_{21}^{\rm net} \approx 1.1\ {\rm s}^{-1}$. The fact that the net damping of the (1,2) mode is so small manifests itself in the size of the fluctuations of the quenched (1,2) mode, while the (2,1) mode is oscillating [Fig. 3(a), 75 s $< t <$ 175 s], that are well above the thermal level ($t <$ 45 s). The dashed curves in the figures show the results of simulations based on numerical integration of Eq. (2), in which the thermal force $F_{\rm th}(t)$ is modeled by means of a memoryless Gaussian stochastic process. As in the experiment, the mode that ultimately oscillates cannot be predicted in advance. The only adjustable parameter in the simulation is the pump laser power, taken to be $P_{\rm in} = 1.18P_{1,2}^{\rm thresh}$.

Figure 3(c) shows a set of trajectories calculated by integrating Eq. (2) with $P_{\rm in} = 1.18P_{1,2}^{\rm thresh}$ for a variety of initial conditions, taking $T = 0$ for clarity. Similar curves were shown in the paper by Lamb [23] in his study of multimode operation of an "optical maser." Corresponding curves for 13 successive realizations of the experiment are shown in Fig. 3(d).

*Anomalous cooling.*—While the amplitudes of the fluctuations in the quenched mode are above the thermal level in Figs. 3(a) and 3(b), the calculated antidamping shown in Fig. 2 shows that we expect cooling of the quenched mode when the amplitude of the oscillating mode is large enough.

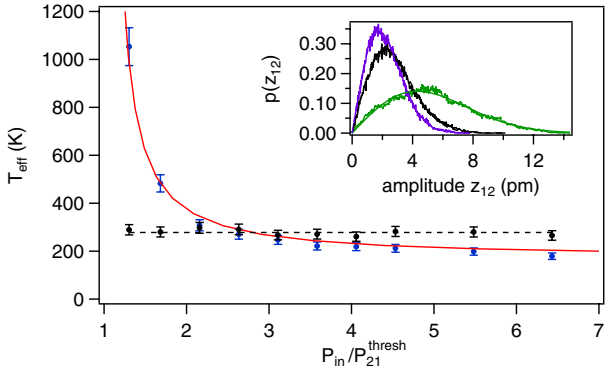


FIG. 4 (color online). Effective temperature of the (1,2) mode while the (2,1) mode oscillates, illustrating anomalous cooling for large pump powers. Black dashed line and circles: temperature inferred without pump $T_0 = 278(21)$ K. Blue circles: effective temperature with pump. Solid red line: analytic prediction $T_{\rm eff} = 293\ {\rm K} \times \Gamma_{12}^{\rm intr}/(\Gamma_{12}^{\rm intr} + \Gamma_{12}^{\rm RP})$. Inset: histograms of the amplitude of the (1,2) mode. Black curve: no pump. Green curve: weak pump $P_{\rm in} = 1.3P_{2,1}^{\rm thresh}$. Violet curve: strong pump $P_{\rm in} = 6.4P_{2,1}^{\rm thresh}$.

To study this matter, we set the (2,1) mode into oscillation with a sequence of ten pump powers from $P_{\rm in} = 1.3P_{2,1}^{\rm thresh}$ to $P_{\rm in} = 6.4P_{2,1}^{\rm thresh}$. For each power, we measured the amplitude $z_{mn}(t)$ of both the (1,2) and (2,1) modes for 450 s, then extinguished the pump, allowed the transients to die away, and measured the thermal amplitudes for another 450 s. The inset to Fig. 4 shows histograms of the amplitudes $z_{12}(t)$ for the cases of no pump, low ($P_{\rm in} = 1.3P_{2,1}^{\rm thresh}$) pump powers, and high ($P_{\rm in} = 6.4P_{2,1}^{\rm thresh}$) pump powers. In thermal equilibrium, the amplitude $z_{mn}$ is distributed according to a Boltzmann distribution

$$p(z_{mn}) = \frac{m_{\rm eff}\omega_{mn}^2}{k_B T} z_{mn} e^{-[(m_{\rm eff}\omega_{mn}^2 z_{mn}^2)/2k_B T]}. \qquad (3)$$

Each of the curves in the inset is fit to Eq. (3). The statistics of the set of ten such thermal (pump off) measurements yields a mean of $T_0 = 278$ K with a standard deviation of $\approx$12 K. The largest uncertainty in the inferred temperature arises from $\phi_{12}(x_0, y_0)$, used to infer $z_{12}(t)$, and contributes an uncertainty of 6%; adding the statistical contribution in quadrature, we assign an uncertainty of 7.5% to the temperature measurements. At $P_{\rm in} = 1.3P_{2,1}^{\rm thresh}$, the statistics of the fluctuations in the (1,2) mode, while the (2,1) mode is oscillating, correspond to an effective temperature of 1040(77) K. At $P_{\rm in} = 6.4P_{2,1}^{\rm thresh}$, the effective temperature is 180(14) K, illustrating the anomalous cooling predicted in Fig. 2. Figure 4 shows the effective temperature inferred from fits to Eq. (3) for all ten pump powers. Also shown is the analytic prediction $T_{\rm eff} = 293{\rm K} \times \Gamma_{12}^{\rm intr}/(\Gamma_{12}^{\rm intr} + \Gamma_{12}^{\rm RP})$ [16].

*Conclusion.*—We have studied the problem of mode competition in a multimode phonon laser both theoretically and experimentally. By using a highly reflective membrane

as the end mirror of an optical cavity, in which many mechanical modes are coupled to the intracavity radiation pressure, we demonstrate that the oscillation of one mode tends to "steal" gain from more weakly oscillating modes, culminating in single-mode steady-state operation. Remarkably, the strong oscillation of one mode even causes optical damping of the other modes. In addition to more fully illuminating the analogy between phonon lasers and their optical counterparts, the insights gained here can be used to force a particular mode to oscillate when multiple modes are capable of oscillation, which may be useful as applications of phonon lasers appear.

We acknowledge useful discussions with Jake Taylor and support from the National Science Foundation through the Physics Frontier Center at the Joint Quantum Institute. Research was performed in part at the NIST Center for Nanoscale Science and Technology.

[1] E. B. Tucker, Phys. Rev. Lett. **6**, 547 (1961).
[2] E. M. Ganapolskii and D. N. Makovetskii, Solid State Commun. **15**, 1249 (1974).
[3] E. M. Ganapolskii and D. N. Makovetskii, Solid State Commun. **90**, 501 (1994).
[4] H. Liu, C. Song, Z. Wasilewski, A. SpringThorpe, J. Cao, C. Dharma-wardana, G. Aers, D. Lockwood, and J. Gupta, Phys. Rev. Lett. **90**, 077402 (2003).
[5] S. S. Makler, M. I. Vasilevskiy, E. V. Anda, D. E. Tuyarot, J. Weberszpil, and H. M. Pastawski, J. Phys. Condens. Matter **10**, 5905 (1998).
[6] I. Camps, S. Makler, H. Pastawski, and L. Foa Torres, Phys. Rev. B **64**, 125311 (2001).
[7] A. Kent, R. Kini, N. Stanton, M. Henini, B. Glavin, V. Kochelap, and T. Linnik, Phys. Rev. Lett. **96**, 215504 (2006).
[8] R. P. Beardsley, A. V. Akimov, M. Henini, and A. J. Kent, Phys. Rev. Lett. **104**, 085501 (2010).
[9] M. Trigo, A. Bruchhausen, A. Fainstein, B. Jusserand, and V. Thierry-Mieg, Phys. Rev. Lett. **89**, 227402 (2002).
[10] L. Tilstra, A. Arts, and H. de Wijn, Phys. Rev. B **68**, 144302 (2003).
[11] L. Tilstra, A. Arts, and H. de Wijn, Phys. Rev. B **76**, 024302 (2007).
[12] K. Vahala, M. Herrmann, S. Knünz, V. Batteiger, G. Saathoff, T. W. Hänsch, and T. Udem, Nat. Phys. **5**, 682 (2009).
[13] J. B. Khurgin, M. W. Pruessner, T. H. Stievater, and W. S. Rabinovich, Phys. Rev. Lett. **108**, 223904 (2012).
[14] M. Bagheri, M. Poot, M. Li, W. P. H. Pernice, and H. X. Tang, Nat. Nanotechnol. **6**, 726 (2011).
[15] C. Metzger, M. Ludwig, C. Neuenhahn, A. Ortlieb, I. Favero, K. Karrai, and F. Marquardt, Phys. Rev. Lett. **101**, 133903 (2008).
[16] T. J. Kippenberg and K. J. Vahala, Opt. Express **15**, 17172 (2007).
[17] I. S. Grudinin, H. Lee, O. Painter, and K. J. Vahala, Phys. Rev. Lett. **104**, 083901 (2010).
[18] H. Okamoto, D. Ito, K. Onomitsu, H. Sanada, H. Gotoh, T. Sogawa, and H. Yamaguchi, Phys. Rev. Lett. **106**, 036801 (2011).
[19] I. Bargatin and M. Roukes, Phys. Rev. Lett. **91**, 138302 (2003).
[20] S. D. Bennett and A. A. Clerk, Phys. Rev. B **74**, 201301 (2006).
[21] I. Mahboob, K. Nishiguchi, A. Fujiwara, and H. Yamaguchi, Phys. Rev. Lett. **110**, 127202 (2013).
[22] S. Knünz, M. Herrmann, V. Batteiger, G. Saathoff, T. Hänsch, K. Vahala, and T. Udem, Phys. Rev. Lett. **105**, 013004 (2010).
[23] W. E. Lamb, Phys. Rev. **134**, A1429 (1964).
[24] A. Siegman, *Lasers* (University Science Books, Sausalito, CA, 1986).
[25] H. Haken, Rev. Mod. Phys. **47**, 67 (1975).
[26] U. Kemiktarak, M. Metcalfe, M. Durand, and J. Lawall, Appl. Phys. Lett. **100**, 061124 (2012).
[27] U. Kemiktarak, M. Durand, M. Metcalfe, and J. Lawall, New J. Phys. **14**, 125010 (2012).
[28] S. Timoshenko, *Vibration Problems in Engineering* (D. Van Nostrand, New York, 1937).
[29] See Supplemental Material at http://link.aps.org/supplemental/10.1103/PhysRevLett.113.030802 for details of the calculation.